

# Electromechanical Analysis of Low Voltage Faults in a Magnetically Coupled Synchronous Generator Set

O. R. Tweedy, Y. Akcay, P. Giangrande, M. Galea, S. D. Garvey

**Abstract** – This paper investigates the magneto-mechanical performance of a magnetically coupled, engine driven synchronous generator set exposed to a severe low voltage grid fault. A multi-physics model of a generator, coaxial magnetic coupling and diesel engine is subjected to a 100% voltage drop scenario and the mechanical response is analysed. The peak coupling torque is significantly lower than that of a generator set coupled with a standard rubber flexible coupling, but the time required for generator to grid resynchronisation is increased. As a result, the machine shafts are protected from severe stress transients that can lead to structural failure. An oversized coaxial magnetic coupling is also analysed to determine the relationship between peak coupling torque and fault ride through performance.

**Index Terms**— fault torque, generator set, low voltage ride through, magnetic coupling, multi-physics model, rotor slip.

## I. INTRODUCTION

In 2021, renewable energy generation made up 42.8% of the total power generation in the UK at its peak during the last quarter of the year [1]. In 2017 the proportion of renewable energy generated peaked at 26.6% during the first quarter of the year [2]. As the proportion of distributed renewable energy increases, the capacity of the grid to maintain stability during low voltage faults reduces [3], [4], particularly in the absence of adequate energy storage and smart grid solutions. This has increased the chance of supply interruptions such as a loss of generation from a wind farm in the event of cascade tripping of wind turbines. The resulting reduction in the total inertia of generating equipment connected to the grid increases the frequency of grid dynamics and plays a significant role in reducing the stability of the system [5]. Given the trend of increasing renewable energy generation, and ever increasing global power demands, it is becoming more important to address the impact of grid instability on grid connected generators to maintain their reliability. In response to these new challenges, modern electricity grid codes specify minimum fault ride through (FRT) time periods for various levels of voltage drop and recovery during which generators must remain connected to the grid [6], [7]. This ensures that power is supplied to the

network during the fault, and once the fault is cleared, all connected generators return to normal operation in synchronism with the grid, thus reducing the chance of brown outs or complete black outs.

Modern generators are designed to remain connected to the grid during low voltage faults in order to maintain grid stability once the electrical fault has cleared [6], [8], [9], and are therefore directly subjected to the associated current and torque transients. Voltage drops of up to 100% can occur over short periods (100's of milliseconds) which subjects the connected generators to the most severe fault condition, equivalent to a three-phase short circuit. The situation where a generator remains connected throughout the duration of the fault is known as low voltage ride through (LVRT).

The resulting shaft torque between the generator and the prime mover can exceed twelve times the steady state torque value depending on the type of coupling used and the ratio of inertia between the prime mover and the generator [10]. Transient fault torques of this magnitude can result in severe damage to the coupling and generator shafts, either due to fatigue from several fault events or in extreme cases, a single large torque transient [10].

Generator sets (gensets) consist of a generator and prime mover, typically connected by flexible couplings (FCs) which allow for some angular displacement between the rotors in order to dampen torsional vibrations and accommodate small shaft misalignments. Such couplings provide a physical mechanical connection and will thus transfer any fault torque from one side, directly to the other. Magnetic couplings (MCs) present a possible solution to eliminate high magnitude torque transients, as they are incapable of transmitting torque of a magnitude above their peak rated torque. If a torque is applied to either side of the MC which exceeds the peak torque value, the rotors will slip relative to one another [11].

In this paper, a multi-physics model of an engine driven synchronous generator set (genset) is subjected to an LVRT event that suddenly reduces the supply voltage to 0 V. The resulting shaft torque and resynchronisation time of the genset is compared when the two machines are coupled with either a flexible coupling or a coaxial magnetic coupling (CMC). The

---

This project received funding from the Clean Sky 2 Joint Undertaking under the European Union's Horizon 2020 research and innovation programme under grant agreements no 821023 and no. 807081. This work was also partially funded by the University of Nottingham Propulsion Futures Beacon.

O. R. Tweedy, Y. Akcay, P. Giangrande and M. Galea are with the Power Electronics, Machines and Control Group, and S. D. Garvey is with the Gas Turbines and Transmissions Research Group, The University of Nottingham, NG7 2GT, UK (e-mail: oliver.tweedy1@nottingham.ac.uk).

work builds on existing research on magnetic coupling design [12], [13] and slip behavior under transient conditions [11], and investigates an application within a real-world scenario. The introduction of a CMC for a low voltage fault scenario reveals its advantages and disadvantages, which are discussed and analysed in the following.

## II. SPECIFICATIONS AND GEOMETRY

### A. Electromagnetic Generator Model

The generator studied in this paper is a four pole synchronous generator rated at 72.5 kVA. It produces 58 kW of electrical power at full load operation with a lagging power factor of 0.8. The electromagnetic model of the generator was built using ANSYS Maxwell, as done in [14]. This model consists of a 2-D slice through the generator, including the rotor, stator, windings, damper cage and support bars as shown in Fig. 1. The stator windings are divided into three phase windings, each with two branches that are arranged around the stator. The stator circuit is connected in series star (wye) configuration with the supply grid circuit which is external to the generator sub-model. The specifications of the generator are listed in Table I.

The generator model was experimentally validated against the results collected during an actual three-phase short circuit test performed on the generator. To run the model at steady state conditions, the rotational speed was set to 1500 RPM and the field current was set to 23 A using a pre-set current versus time curve applied directly to the rotor windings. This induced the rated generator current with each phase from the stator connected to a voltage supply representing the electrical grid, thus producing an electromagnetic torque of 370 Nm, equal to the rated load of the generator. The supply voltage is ramped up over a period of 300 ms to achieve stable steady state operation. To simulate the short circuit, the supply voltage was suddenly reduced to 0 V after the simulation had reached steady state. At the same time, the field current was increased to 250 A over a period of 14 ms and reduced back to 23 A over a period of 20 ms to force a current transient in the stator equal to that which would be produced by the real three-phase short circuit. This is done so that the same current inrush could be reproduced in the later LVRT simulations without shorting the phases in the model. In the LVRT case, there is no physical short and the generator terminals must remain connected to the grid supply. The generator model was also tested when connected to a circuit with a resistive load, rather than the grid voltage supply and the phases were suddenly shorted together via switches. The resulting stator current and voltage response was identical to the sudden voltage drop case on the supply. The amplitude and period of the increased field current was manually adjusted to account for the fault current until the current and torque results matched the experimental results. The torque and current results from the moment the short circuit is simulated are summarised in Fig. 2 and Fig. 3 respectively. The initial peak phase voltage prior to the short circuit is 311 V which corresponds to 220 V *rms*, thus a 3-phase voltage of 380 V for a wye terminal connection. The current results are not exactly matched as they are highly

sensitive to the precise value and phase of the voltage at the moment the short is applied. However, the average amplitude and period of the first peak in each phase is within acceptable limits as the first peak of the torque shown in Fig. 2 is just 1.2% lower than the experimentally obtained value of 2.7 kNm. Since a 100% voltage drop fault is equivalent to a 3-phase short circuit fault in terms of the peak current, voltage and therefore electromagnetic torque produced by the generator, the model will also react as the real machine would to a low voltage fault. Note that the automatic voltage regulator (AVR) for the generator was active in the experimental 3-phase short circuit test but its function is not included in this simulation. In this case the voltage is manually controlled using the field current curve. Any influence that the AVR has on the stator current is therefore automatically reproduced in the results when the field current is adjusted to match the simulated current with the experimental current. The same is true for the exciter which was also present and active in the experiment but not included in the model.

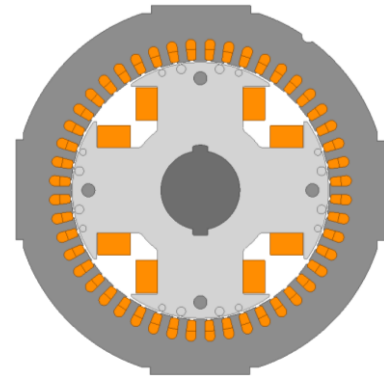


Fig. 1. 2D geometry of the synchronous generator

TABLE I. GENERATOR SPECIFICATIONS AND DIMENSIONS

Specification	Value
Rated Power (kW)	58
Rated Voltage (V)	380
Rated Current (A)	190
Rated Speed (RPM)	1500
Rated Torque (Nm)	370
Rotor Inertia (kg.m <sup>2</sup> )	0.56
Rotor Mass (kg)	102.3

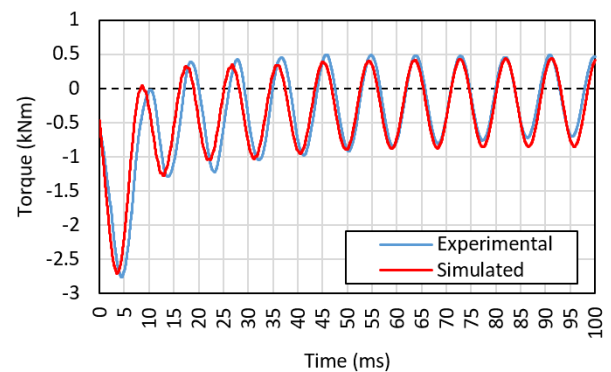


Fig. 2. Model experimental validation: shaft torque waveforms following a three-phase short circuit

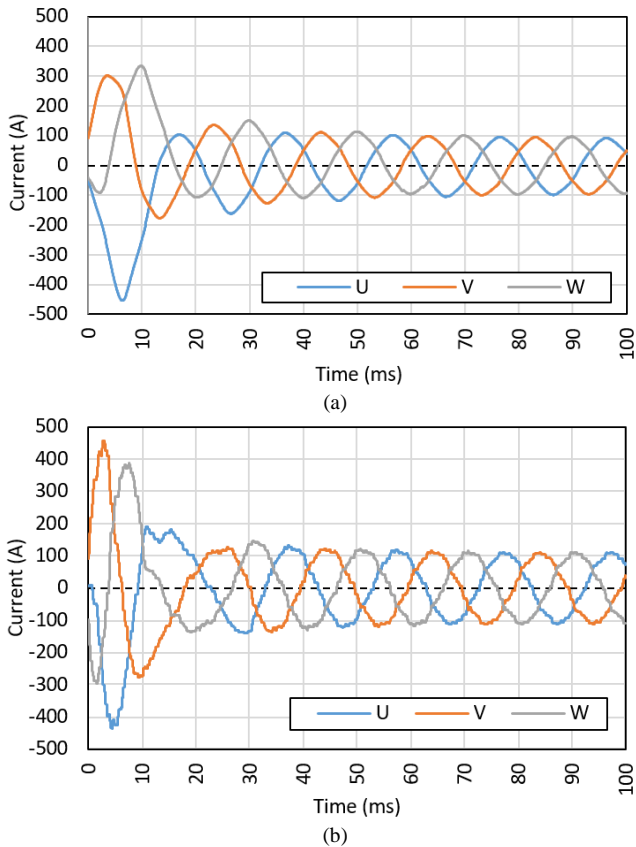


Fig. 3. Generator model experimental validation: current waveforms following a three-phase short circuit; (a) experimental results, (b) simulation results

### B. Electromagnetic CMC Model

The CMC model is composed of inner and an outer magnet rotor geometries capable of transmitting a peak torque of 400 Nm with an axial length of 116.5 mm. The CMC is designed based on the generator's requirements with a slightly higher peak torque capability for a safety margin. The CMC has 32 permanent magnet pole pairs in total and an airgap thickness of 2.5 mm. The permanent magnet material was set to neodymium N40/23 and the back iron material of both the rotor and stator was set to electrical steel M43. The CMC model geometry is shown in Fig. 4 and the specifications of the model are listed in Table II.

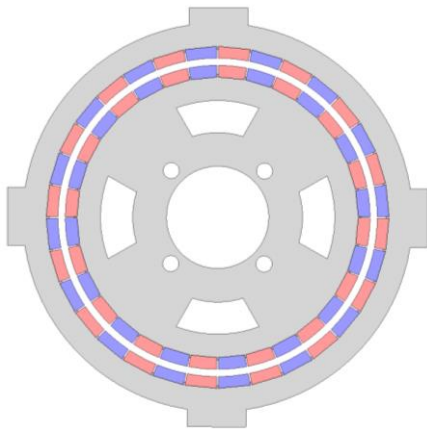


Fig. 4. 2D geometry of the CMC

TABLE II. CMC SPECIFICATIONS AND DIMENSIONS

Specification	Value
Torque (Nm)	400
Pole-Pair Number	32
Air-gap Thickness (mm)	2.5
Axial Length (mm)	116.5
Inner Magnet Diameter (mm)	104
Inner Rotor Inertia (kg.m <sup>2</sup> )	0.09
Outer Rotor Inertia (kg.m <sup>2</sup> )	0.02

### C. Multi-Physics Model

The multi-physics model is composed of a transient electromagnetic model of the generator, a transient electromagnetic model of the CMC and a 1D torsional mechanical model of the full generator set connected together using ANSYS Simplorer. The 1D torsional model used in the following analyses is based on (1), which is derived from the general equation of motion and expanded for all components in the assembly.

$$I(\ddot{\theta}(t)) + C(\dot{\theta}(t)) + k_T(\theta(t)) = T(t) \quad (1)$$

where  $\theta$ ,  $\dot{\theta}$ , and  $\ddot{\theta}$  are angular displacement, angular velocity, and angular acceleration respectively.  $I$  is the mass moment of inertia about the axis of rotation ( $z$ ),  $C$  is the torsional damping factor and  $T$  is the applied torque. The torsional stiffness  $k_T$  of each spring element in the 1D model is obtained using (2).

$$k_T = \frac{GJ}{l} = \frac{T}{\theta} \quad (2)$$

where  $G$  is the shear modulus,  $J$  is the area moment of inertia about the  $z$ -axis, and  $l$  is the length of the element.

The shear modulus, and therefore the torsional stiffness of the laminated rotor core, is determined by matching the modal frequencies and shapes obtained from a parametric modal analysis of a 3-D model of the rotor with those obtained from a modal test performed on the real rotor [14].

The engine driven synchronous generator set consists of a 1D torsional model of the generator and engine rotors, with the generator side of the model connected to a 2D transient magnetic model of the generator rotor and stator. Torque and speed values are communicated between the electromagnetic and mechanical models. The engine side is connected to a simple PI controller representing the governor/speed control of the engine.

The CMC is similarly represented by a 2D transient magnetic model of the coupling connected to a 1D torsional model of both the inner and outer magnet rotors. The inner and outer rotor inertias are connected to the generator and engine torsional models respectively. The complete CMC coupled genset model is capable of simulating a range of electrical and mechanical faults. A system overview for the multi-physics model is presented in Fig. 5. Note that the generator set in this simulation does not include any LVRT protection systems such as braking resistors, thus the resulting peak transient electromagnetic torque is very large.

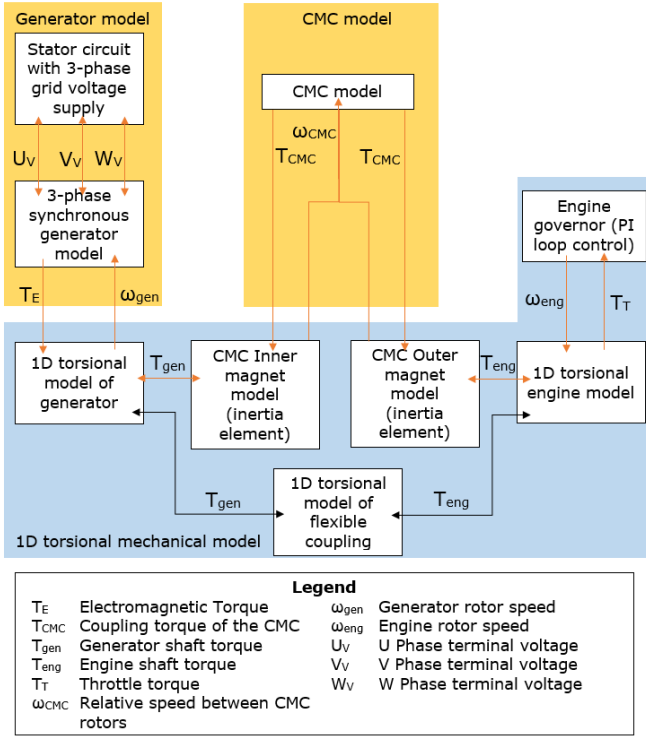


Fig. 5. Multi-physics model system overview of the magnetically coupled generator set

The maximum torsional stiffness of the CMC,  $k_{Tmax}$ , is obtained using (3).

$$k_{Tmax} = \frac{T_{pk}}{\theta_{max}} \quad (3)$$

where  $T_{pk}$  is the peak coupling torque (400 Nm) and  $\theta_{max}$  is the maximum relative angular displacement (0.1 rads, 5.63 degrees) between the magnets. The values for which are obtained from a transient electromagnetic simulation of the CMC model.

The flexible coupling is based on a HTB-GS flexible coupling [15] (size 4000) with a maximum torsional stiffness of 0.549 MNm/rad (at 4000 Nm, 100% rated load). Such couplings are commonly used in gensets of this size. As one would expect, the maximum torsional stiffness of the CMC is far lower than that of even a flexible rubber coupling due to the lack of a physical interface.

Table III shows the torsional stiffness and inertia properties of all 1D torsional elements in the multi-physics model. Fig 6 shows the position of each element in the generator set.

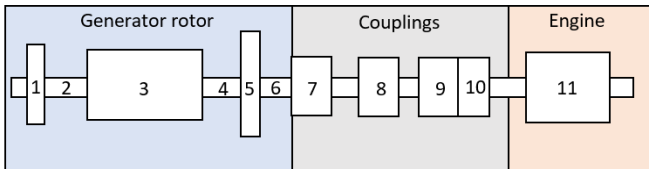


Fig. 6. Component positions within the generator set model as per Table III. Element 7 represents either the FC or the CMC.

TABLE III. 1D TORSIONAL MODEL PROPERTIES

Component	Position	Torsional Stiffness (MNm/rad)	Mass Moment of Inertia (kg.m <sup>2</sup> )
Exciter	1	0.537	0.051
Shaft Section 1	2	2.89	0.003
Generator Core	3	1.2	0.472
Shaft Section 2	4	4.42	0.002
Fan	5	3.02	0.028
Shaft Section 3	6	3.89	0.001
FC	7	0.549	0.4
CMC	7	0.004	0.11
Transducer	8	1.17	0.005
Coupling 1	9	1.17	0.069
Coupling 2	10	1.18	0.04
Engine	11	2.00	1.2

### III. SIMULATION RESULTS

This section presents the key results from analysis of the multi-physics genset model.

#### A. Typical FRT Response of a Grid Connected Generator Set

The electromechanical response of a grid connected synchronous generator set can be summarised as follows. At the onset of a low voltage fault on the electrical grid, a large electromagnetic torque transient is incepted due to the high currents drained by the low overall impedance. This transient electromagnetic torque briefly decelerates the rotor before dropping back to a level determined by the remaining grid voltage and rotor speed. However, the engine still provides the same driving torque as before the failure condition, causing an acceleration of the generator. The acceleration continues until the engine governor corrects the genset speed back to the target level. During this time, the grid voltage may be restored causing an additional electromagnetic torque transient, which may be even greater than the previous depending on the angle of slip reached between the rotors in the FRT period.

The following analyses focus on the case of a sudden low voltage fault occurring in the electrical grid to which the generator is connected. Two mechanical connection cases are evaluated: 1) through flexible coupling and 2) via the CMC. The results are compared and the low voltage fault ride through performance of the CMC coupled genset is evaluated.

#### B. Initial Conditions and Voltage Curve

The initial rotational speed of all elements within the 1D torsional model is set to the rated speed of 157 rad/s (1500 RPM) and the generator output is ramped up to no-load conditions before a load is applied. A gentle increase in generator electromagnetic torque and engine torque is required to start the genset simulation to maintain synchronism between the CMC rotors without incurring slip. In this case the generator rotor field current is ramped from 0 A to 23 A over 300 ms to produce the rated load.

To simulate the low voltage fault, the grid/supply voltage follows the voltage curve shown in Fig. 7. A sudden voltage drop from 311 V (peak) to 0 V occurs at the 700 ms mark, and remains at 0 V for 140 ms, before immediately being restored to 311 V. The results plots for all following figures begin after

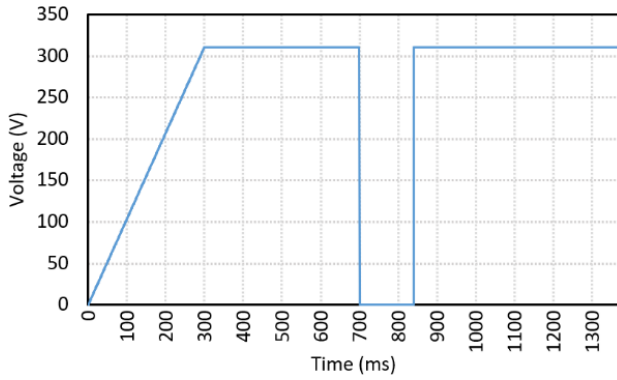


Fig. 7. Pre-set LVRT grid supply peak phase voltage fault curve

steady state conditions are reached.

The inertia of the generator core is increased to  $1.2 \text{ kg.m}^2$  to represent a generator set where the ratio of inertias between machines is low.

### C. CMC and FC Performance Comparison

Comparisons between the FC and CMC models can be made from the following figures. Most important is the coupling torque that is measured at either side of the couplings. Fig. 8a shows that the peak transient torque transmitted to the engine and generator during the initial voltage drop and subsequent voltage restoration is greatly reduced by 89.5%. However, due to the transient torque exceeding the peak torque capacity of the CMC, the magnet rotors slip relative to one another, resulting in a 400 Nm torsional vibration throughout the FRT period and for a time following fault clearance.

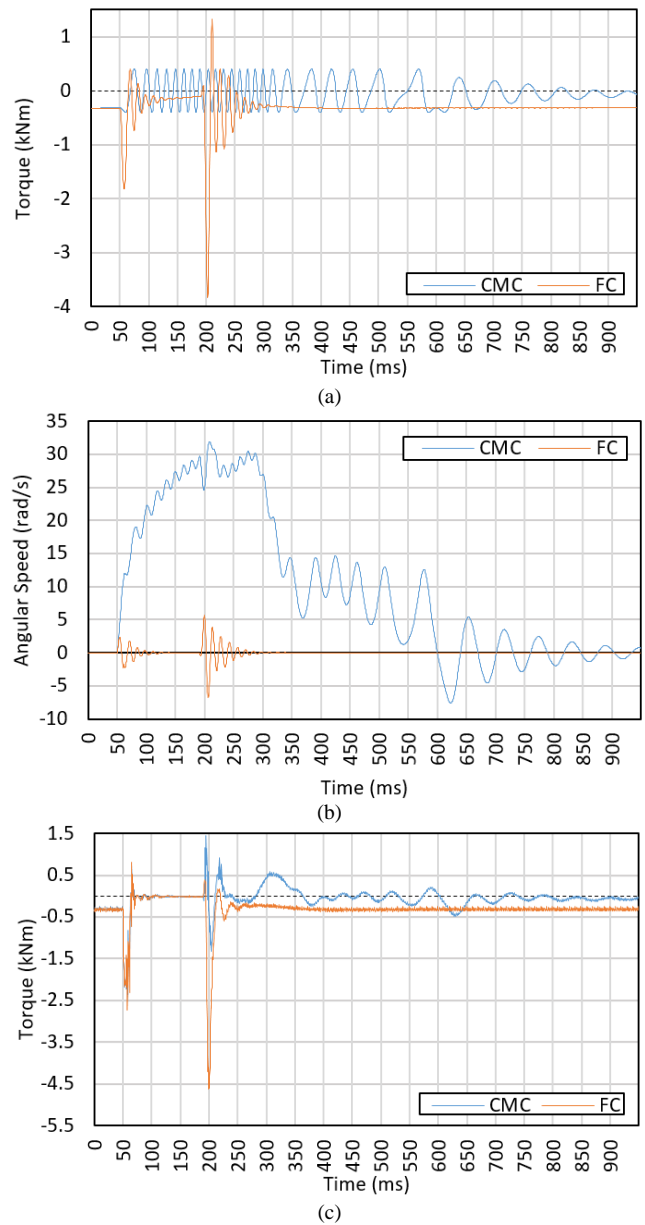
As the supply voltage is immediately restored at 840 ms, the electromagnetic torque transient is maximised. The magnitude of electromagnetic torque at this point differs between the FC and CMC models as the peak electromagnetic torque depends on the precise relative angular position between the generator rotor and stator the moment that the supply is restored. Therefore, should the fault time be extended, rotor inertias change, the level of voltage drop, or several other factors change between simulations, the peak torque will change dramatically. In this case the maximum fault electromagnetic torque achievable with this generator model is 7 kNm [14].

The relative angle shown in Fig. 8b is different between the FC and CMC simulations due to slip and the resulting increase in engine acceleration and generator deceleration in the CMC case. The rotors are incapable of slipping in the FC case. The CMC rotors will only stop slipping once the speed on both rotors is equal and the transmitted torque is lower than the peak torque. In this case, the CMC will stop slipping once the engine governor (the PI control) corrects the engine speed.

The approximate time at which the CMC rotors stop slipping and resynchronise may be obtained from Fig. 8b where the relative speed between the engine and generator crosses 0 rad/s. The resynchronisation time can also be obtained from the double peak shown in Fig. 8a, which occurs at the 600 ms mark. The FC on the other hand does not lose

synchronism between the two rotors but will still require a short period for the speed of the full system to return to 157 rad/s. Fig. 8c compares the electromagnetic torque produced by the generator for both CMC and FC cases and Fig. 8d shows the angular speed of the generator and engine rotors for the CMC case alone.

The peak torque of the FC coupled genset at the initial point of voltage drop is 1.81 kNm and is 3.8 kNm at the point of voltage restoration. The CMC on the other hand limits the peak torque to 0.4 kNm at both points. The electromagnetic torque is reduced by 72% as the relative angular shift of the generator rotor between its steady state position and its actual position is approximately  $45^\circ$ . During LVRT, the relative angular speed between the generator and engine reaches a maximum of 32 rad/s as the generator speed drops to 140 rad/s (1336.9 RPM) and the engine speed increases to 172 rad/s (1642.5 RPM).



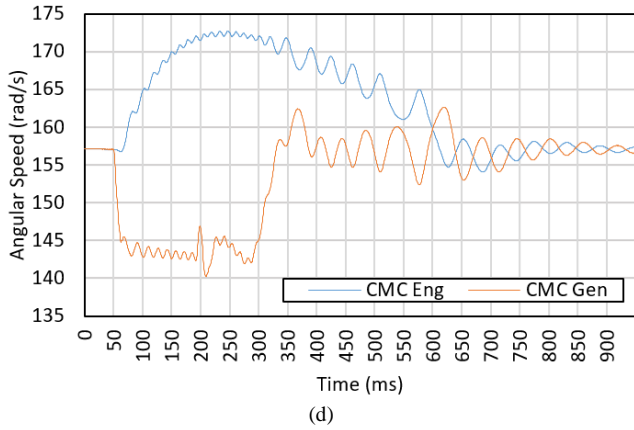


Fig. 8. LVRT simulation results for CMC and FC coupled genset models; (a) coupling torque, (b) relative angular speed between the generator and engine, (c) generator electromagnetic torque, (d) angular speed of the generator and engine for the CMC connected model.

#### D. CMC Size Comparison

A comparison of fault performance versus CMC peak torque is made to determine how the selection of CMC size influences the reconnection behavior of the generator. The resynchronisation time is measured between the instant of grid voltage restoration and the moment when the engine and generator speeds match. This moment is identified by the double peak in the coupling torque results. The key results of the comparison are shown in Table IV. The 1000 Nm CMC is simulated by extending the axial length of the CMC model to 291 mm.

TABLE IV. LVRT PERFORMANCE FOR DIFFERENT SIZED CMCs

CMC Peak Torque (Nm)	Maximum Relative Speed (rad/s)	Resynchronisation Time (ms)	Peak Shaft Stress (Mpa)
1000	31.7	360	30.6
400	32	410	12.2

The minimum shear yield limit for an EN8 medium carbon steel shaft is 140 MPa (50% of the 280 MPa tensile yield strength). Beyond this stress, the shaft is at risk of permanent deformation. The shaft diameter is 55 mm. This limit applies to both the generator and engine shafts. The peak shaft shear stress,  $\tau_{shaft}$ , is obtained using (4).

$$\tau_{shaft} = \frac{Tr}{J} \quad (4)$$

where  $r$  is the radius of the shaft (27.5 mm).

The fatigue limit for infinite life for medium carbon steels is around 270 MPa according to standard material S-N curves. Therefore, the fatigue limit under shear loading is 135 MPa here. Provided that  $\tau_{shaft}$  remains below this value, the machine shafts will not fail under cyclical loading such as torsional vibration due to magnet slip. With the CMC rotors coupled directly to the genset shafts (press fit, fully bonded connection), the peak shaft shear stress is 12.2 MPa for the 400 Nm CMC genset and 116.3 MPa for the FC genset.

## IV. CONCLUSIONS

The multi-physics model developed here allows for the simulation of CMCs within diesel engine driven synchronous generator sets and demonstrates the performance of CMCs when subjected to severe fault events such as LVRT. When the genset is coupled with a CMC (400 Nm peak torque), the peak torque transient at the beginning of the fault is reduced by 77.9% and the torque transient at the point of grid reconnection is reduced by 89.5% compared to when a rubber flexible coupling is used. The peak stress in the shafts of the generator and the engine is consequently reduced by 89.5%. The peak shear stress in the FC model is 83% of the shear yield limit which is particularly dangerous considering that it is possible for the peak coupling torque to exceed the 3.8 kNm obtained in this simulation. The 1000 Nm CMC achieves resynchronisation 50 ms earlier than the 400 Nm CMC, but increases the peak coupling torque and the magnitude of torsional vibration.

The main advantage of using an oversized CMC would be to prevent slip for smaller grid faults just above the rated torque. The main drawback with using a CMC is that a longer period of resynchronisation is required after the fault has cleared, which may not meet grid code regulations. This is not as much of a problem for a standalone genset.

Another side-effect of the CMC is the torsional vibration that occurs when the peak torque is exceeded. The oscillating load on connected machinery can loosen assemblies and reduce the life of connected subcomponents such as rotor windings, whilst a significant amount of heat is generated due to eddy current formation in the back iron of the CMC rotors leading to thermal management issues. Ultimately, the overall LVRT performance of the CMC coupled genset is reduced, but the risk of physical rotor damage is greatly reduced.

The results obtained here indicate the relative impact that a magnetic coupling has on the generator set during LVRT. Further validation is required from an experimental LVRT test to compare the fault performance of a flexible coupling and a magnetic coupling.

## V. ACKNOWLEDGMENT

This project received funding from the Clean Sky 2 Joint Undertaking under the European Union's Horizon 2020 research and innovation programme under grant agreements no 821023 and no. 807081. This work was also partially funded by the University of Nottingham Propulsion Futures Beacon.

## VI. REFERENCES

- [1] K. Harris, 'Energy Trends. UK, October to December 2021 and 2021'. Department for Business, Energy & Industrial Strategy, Mar. 31, 2022. Accessed: Jun. 09, 2022. [Online]. Available: [https://assets.publishing.service.gov.uk/government/uploads/system/uploads/attachment\\_data/file/1064782/Energy\\_Trends\\_March\\_2022.pdf](https://assets.publishing.service.gov.uk/government/uploads/system/uploads/attachment_data/file/1064782/Energy_Trends_March_2022.pdf)
- [2] K. Harris, 'Energy Trends. June 2017'. Department for Business, Energy & Industrial Strategy, Jul. 29, 2017. Accessed: Jun. 09, 2022. [Online]. Available: <https://assets.publishing.service.gov.uk/government/uploads/system/u>

- ploads/attachment\_data/file/639098/Energy\_Trends\_June\_2017.pdf
- [3] H. Johal, R. Konopinski, J. Skliutas, M. Eitzmann, and D. Leonard, 'Solutions to Improve Grid Code Compliance of Synchronous Generation', presented at the 2014 Grid of the Future Symposium, Houston, Texas, USA, 2014. [Online]. Available: <http://cigre-usnc.org/wp-content/uploads/2015/06/Solutions-to-Improve-Grid-Code-Compliance-of-Synchronous-Generation.pdf>
  - [4] C. Ruester, S. Hoppert, and J. Blum, 'Power Quality and Stability Issues in Modern Distribution Grids: Identification and Mitigation', presented at the CIRED Workshop, Rome, Italy, 2014. [Online]. Available: <https://citeseerx.ist.psu.edu/viewdoc/download?doi=10.1.1.1086.2201&rep=rep1&type=pdf>
  - [5] A. Ulbig, T. S. Borsche, and G. Andersson, 'Impact of Low Rotational Inertia on Power System Stability and Operation', *IFAC Proc. Vol.*, vol. 47, no. 3, pp. 7290–7297, 2014, doi: 10.3182/20140824-6-ZA-1003.02615.
  - [6] M. Östman, N. Wägar, I. Ristolainen, and J. Klimstra, 'The impact of grid dynamics on low voltage ride through capabilities of generators', presented at the PowerGrid Europe 2010, Amsterdam, Netherlands, 2010. [Online]. Available: [https://www.researchgate.net/publication/234128171\\_The\\_impact\\_of\\_grid\\_dynamics\\_on\\_low\\_voltage\\_ride\\_through\\_capabilities\\_of\\_generators](https://www.researchgate.net/publication/234128171_The_impact_of_grid_dynamics_on_low_voltage_ride_through_capabilities_of_generators)
  - [7] D. Popovic and I. Wallace, 'International Review of Fault Ride Through for Conventional Generators'. EirGrid, 2010. Accessed: Mar. 04, 2020. [Online]. Available: [http://www.eirgridgroup.com/site-files/library/EirGrid/MPID215\\_FRT\\_KEMA\\_Report\\_16010829.pdf](http://www.eirgridgroup.com/site-files/library/EirGrid/MPID215_FRT_KEMA_Report_16010829.pdf)
  - [8] Y. Shicong, G. V. Shagar, A. Ukil, S. D. G. Jayasinghe, and A. K. Gupta, 'Evaluation of Low Voltage Ride-Through capability of synchronous generator connected to a grid', in *2015 IEEE Power & Energy Society General Meeting*, Denver, CO, USA, 2015, pp. 1–5.
  - [9] A. Michaelides and N. L. Brown, 'CyberGen: modelling the design challenges for small embedded synchronous generators connected to increasingly unstable networks', in *5th IET International Conference on Power Electronics, Machines and Drives (PEMD 2010)*, Brighton, UK, 2010, pp. 435–435.
  - [10] S. Narayanan, G. Berridge, A. Biebhaghauser, and N. L. Brown, 'Fault Ride through Effects on Alternators Connected to the Grid.' Cummins Generator Technologies, 2012. Accessed: Mar. 04, 2020. [Online]. Available: [http://www.gridcodegenerators.com/library/LVRT\\_Grid\\_White\\_Paper\\_EN\\_LR.pdf](http://www.gridcodegenerators.com/library/LVRT_Grid_White_Paper_EN_LR.pdf)
  - [11] T. Lubin, S. Mezani, and A. Rezzoug, 'Experimental and Theoretical Analyses of Axial Magnetic Coupling Under Steady-State and Transient Operations', *IEEE Trans. Ind. Electron.*, vol. 61, no. 8, pp. 4356–4365, Aug. 2014, doi: 10.1109/TIE.2013.2266087.
  - [12] Y. Akcay, P. Giangrande, and M. Galea, 'Design, Analysis and Dynamic Performance of Radial Magnetic Coupling', in *2020 23rd International Conference on Electrical Machines and Systems (ICEMS)*, Hamamatsu, Japan, Nov. 2020, pp. 222–227. doi: 10.23919/ICEMS50442.2020.9291124.
  - [13] Y. Akcay, P. Giangrande, C. Gerada, and M. Galea, 'Comparative Analysis Between Axial and Coaxial Magnetic Couplings', in *The 10th International Conference on Power Electronics, Machines and Drives (PEMD 2020)*, Online Conference, 2021, pp. 385–390. doi: 10.1049/icp.2021.1147.
  - [14] O. Tweedy, 'Multi-Physics Modelling of a Grid Connected Diesel Engine Driven Synchronous Generator Set for the Analysis of Transient Low Voltage Ride Through Performance', Ph.D. dissertation, University of Nottingham, Nottingham, 2021. Accessed: Feb. 08, 2022. [Online]. Available: <https://ethos.bl.uk/OrderDetails.do?uin=uk.bl.ethos.836462>
  - [15] 'HTB-GS, DCB-GS and RB Superior Coupling Technology. Hi-Tec Generator and Pump Set Couplings'. HTB. [Online]. Available: [https://www.renold.com/media/162089/htb\\_gs\\_dcb\\_gs\\_rb\\_new.pdf](https://www.renold.com/media/162089/htb_gs_dcb_gs_rb_new.pdf)

## VII. BIOGRAPHIES

**O. R. Tweedy** received his Ph.D. degree in mechanical engineering from the University of Nottingham, U.K., in

2021. He worked with the Research and Development Department Group at Cummins Generator Technologies, Peterborough, U.K. as a Mechanical Design Engineer before joining the PEMC Group at the University of Nottingham as a Research Fellow in 2020. His main research interests include rotor-dynamic and electromechanical analysis of electrical machines. He is an associate member of the Institution of Mechanical Engineers.

**P. Giangrande** (Senior Member, IEEE) received his Ph.D. degree in electrical engineering from the Politecnico of Bari, in 2011. Since 2012, he has been a Research Fellow with the Power Electronics, Machines, and Control (PEMC) Group, University of Nottingham, U.K. In 2019, he was appointed as a Senior Research Fellow with the PEMC Group, where he is also the Head of the Accelerated Lifetime Testing Laboratory. His main research interests include design and testing of electromechanical actuators for aerospace, thermal management of high-performance electric drives, and reliability of electrical machines.

**Y. Akcay** received his M.Sc. degree in electrical engineering and his Ph.D. degree in electrical and electronic engineering from the University of Nottingham, Nottingham, U.K., in 2014 and 2018, respectively. He is currently a Postdoctoral Research Fellow with the Power Electronics, Machines, and Control Group, University of Nottingham. His main research interests include the design and analysis of the magnetic gearboxes and magnetic couplings for aerospace applications.

**M. Galea** (M'13-SM'18, FRAeS) received his PhD in electrical machines design from the University of Nottingham, UK, where he has also worked as a Research Fellow. He is currently the Head of The School of Aerospace in the University of Nottingham, Ningbo, China, where he is also the Director of Aerospace. He currently lectures in Electrical Drives and in Aerospace Systems Integration and manages a number of diverse projects and programmes related to the more / all electric aircraft, electrified propulsion and associated fields. His main research interests are design, analysis and thermal management of electrical machines and drives (classical and unconventional), the more electric aircraft and electrified and hybrid propulsion. He is a Fellow of the Royal Aeronautical Society and a Senior Member of the IEEE.

**S. D. Garvey** Graduated in 1984 from University College Dublin with a 1st Class Hons Degree in Mech. Eng. He worked for GEC Large Electrical Machines Ltd., Rugby from 1984–1990. He then joined Aston University as a lecturer in Mechanical Engineering. By 1998, he was promoted to Reader in Mechanical Engineering. He left Aston University to join Nottingham University in 2000 as Professor of Dynamics.